NANO LETTERS

2007
Vol. 7, No. 9
2688−2692

Nonequilibrium Quantum Transport Properties of a Silver Atomic Switch

Zhongchang Wang,*,†,‡ Takuya Kadohira,†,‡ Tomofumi Tada,†,‡ and Satoshi Watanabe†,‡

Department of Materials Engineering, The University of Tokyo, 7-3-1 Hongo, Bunkyo-ku, Tokyo 113-8656, Japan, and CREST, Japan Science and Technology Agency, 4-1-8 Honcho, Kawaguchi, Saitama 332-0012, Japan

Received May 11, 2007; Revised Manuscript Received July 23, 2007

ABSTRACT

Combining nonequilibrium Green's function technique with density functional theory, electron transport, and structural properties of an Ag atomic switch through Ag_2S have been investigated. We have found that an Ag atomic conductance channel in Ag_2S is generated after structure optimization, resulting in large enhancement of the electron transmission coefficient at the Fermi level and metallic behavior of the Ag–Ag_2S–Ag system. Such spontaneous metallization at the Ag–Ag_2S interface may play an important role in fast switching of the Ag–Ag_2S atomic switch.

One of the most active fields in nanotechnology research is the development of electronic circuits made of nanoscale components. Several groups have succeeded in fabricating devices such as rectifiers,[1,2] switches,[3,4] and latches[5] in which the active part is a single molecule, a metallic nanowire, or a similar nanoscale structure. Among them, switches have captured considerable attention because they are key elements of both logic and memory circuits. It is essentially important to examine switches through nanowires[6−9] or molecules[10−12] because the appearance of quantum effects makes it difficult to understand and design these nanoscale switches from the knowledge of microelectronic devices.

Recently, Terabe et al. proposed a novel switch fabricated by a mixed ionic conductor Ag_2S.[13,14] This switch has the advantage of having simple device structure, stability and reliability at room temperature and being easy to transfer to real electronic circuits over most of other nanoscale switches.[15,16] In their research, an Ag_2S layer is connected to a battery through two metallic leads (at least one is silver). They speculated that Ag atoms are accumulated at the interface between silver sulfide and the negative electrode and, finally, a conductive Ag bridge inside the Ag_2S segment is generated to make the system switch ON. Switch OFF can be realized by reversing the electrical potential. Though a lot of intriguing results have already been obtained concerning this switch,[13−16] its working mechanism has not been well clarified yet. In addition, it is still unknown what kind of changes (e.g., structural change) induces the metallic nature in the ON state. These points remain unclear because of the following reasons: (1) The Ag_2S region in the atomic switch takes the room-temperature phase (β-phase), while previous researches concerning Ag_2S are focused on the high-temperature phase (α-phase) due to its superionicity.[17,18] (2) Ag−Ag_2S(β-phase) interface structures are still unknown because of the difficulty in direct observation of the interface in experiment, together with the lack of theoretical investigations. (3) The effect of applied bias voltages on atomic structure and electronic properties is also quite hard to investigate both experimentally and theoretically.

Here, as an initial step to clarify its switch mechanism, we have examined atomic structure, electronic states, and electron transport properties of the Ag−Ag_2S(β-phase)−Ag system from first-principles. Note that hereafter Ag_2S indicates the β-phase Ag_2S in this Letter. First, we constructed atomic models of the Ag−Ag_2S interface and examined their relative stabilities. Then, we investigated electronic states and electron transport properties of Ag_2S connected with two Ag electrodes to clarify the physical properties of Ag_2S around the Ag−Ag_2S interface. Unexpectedly, we have found that a zigzag arrangement of Ag atoms is formed in Ag_2S after structure optimization and that the Ag−Ag_2S−Ag system shows metallic characteristics. This is the first report on the spontaneous metallization of Ag_2S at the Ag−Ag_2S interface.

It is known that the room-temperature phase of Ag_2S has a monoclinic structure.[19] As for the Ag−Ag_2S interface, the orientation relationship between Ag and its sulfide was

* Corresponding author. Current address: Department of Materials Engineering, The University of Tokyo, 7-3-1 Hongo, Bunkyo-ku, Tokyo, 113-8656, Japan. E-mail: wang@cello.t.u-tokyo.ac.jp. TEL/ FAX: +81-3-5841-1286.

† Department of Materials Engineering, The University of Tokyo.

‡ CREST, Japan Science and Technology Agency.

10.1021/nl0711054 CCC: $37.00
Published on Web 08/02/2007

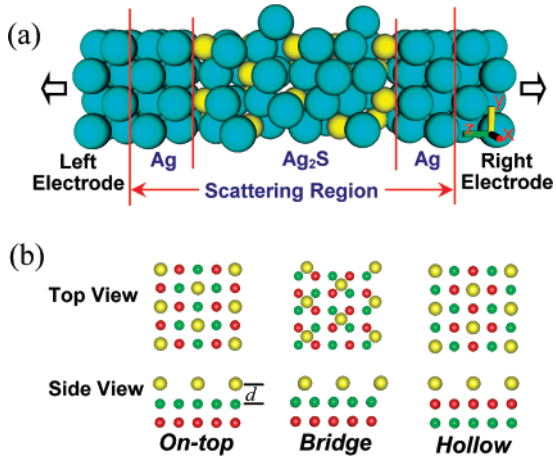

Figure 1. (a) Schematic illustration of the Ag−Ag_2S−Ag system. The yellow balls represent S atoms while green ones represent Ag atoms. (b) The three interface structures investigated: on-top, bridge, and hollow cases.

observed to be (0−12)Ag_2S//(001)Ag and [100]Ag_2S//[100]-Ag by transmission electron microscopy and selected area electron diffraction observation.[20,21] Since no detailed experimental data on atomic arrangement at the Ag−Ag_2S interface are available, we have constructed three models of the interface structure within the above orientation relationship. In the three models, S atoms in the Ag_2S layer proximal to the interface are located at the on-top, bridge, and hollow sites of the outmost layer of Ag electrode, respectively, as shown in Figure 1b. Various cases have also been examined for the junction distance between the Ag electrode and the Ag_2S, *d*.

Figure 1a shows our model of Ag−Ag_2S−Ag system, which can be divided into the left semi-infinite electrode, the scattering region, and the right semi-infinite electrode. The electronic and atomic structures of the semi-infinite electrodes are assumed to be the same as those of the bulk Ag. On the other hand, the electronic states of the scattering region are calculated self-consistently, and atomic relaxation is also examined in some cases. The scattering region consists of monoclinic Ag_2S layers and four (2×2) surface layers of the left and right electrodes. The periodic boundary conditions are imposed in the directions parallel to the interface (*x* and *y* directions). The unit cell of the scattering region consists of 84 atoms, of which 52 atoms are in the Ag_2S layers.

The electronic states and electron transport properties of the above system are explored with the fully self-consistent nonequilibrium Green's function method implemented in TranSIESTA-C code and its latest version, Atomistix ToolKit (ATK) code.[22] This method has been applied to many systems successfully[23] but was applied to heterostructures of metal and solid electrolyte for the first time in this study. It is also noted that to the best of our knowledge, the effects of interface structure, contact distance, and structural optimization on transmission for a bulk material sandwiched to two semi-infinite metallic electrodes have also been reported for the first time in this study, although such effects have already been examined in the cases of atomic and molecular bridges in a vacuum.[24,25] The local density approximation (LDA) and the Troullier−Martins nonlocal pseudopotential are adopted,[26] and the valence electrons are expanded in a numerical atomic-orbital basis set of single zeta plus polarization (SZP). Only Γ-point is employed in the **k**-point sampling in the surface Brillouin zone. For transmission spectra, we have found that an increase in **k** points has little effect. The optimum lattice constant of the room-temperature phase of bulk Ag_2S calculated using the above parameters is 98.95% of the experimental value.[27] The calculated energy band gap is 0.688 eV, which is much smaller than the experimental value of 1.2 eV[28] but close to the calculated values of 0.7 eV by Barman et al.[29] and 0.633 eV by Kashida et al.[19] obtained using the linear muffin-tin orbital method within the LDA. The deviation from the experimental value can be ascribed to the well-known drawback of the density functional theory.

The calculated total energy of the Ag−Ag_2S−Ag system as a function of the contact distance *d* is illustrated in Figure 2a. The three curves in this figure corresponding to the on-top, bridge, and hollow cases are calculated without relaxing structural parameters except the *d*. The calculated total energy of the bridge case is 0.167 and 0.180 eV lower than those of the on-top and hollow cases, respectively, per surface atom. For *d* values that give the minima of the total energies of respective cases, we have also calculated the total energies with relaxing all the atoms in the Ag_2S plus two Ag layers proximal to the two interfaces. The results are also shown in Figure 2a, and we can see that the bridge case remains stable over the on-top and hollow cases by 0.029 and 0.125 eV, respectively, per surface atom.

For the bridge case, the minimum energy corresponds to $d = 1.9$ Å, which is shorter than those for the on-top and hollow cases. This is because S atoms at the interface tend to keep an energetically favorable distance from neighboring Ag atoms. For the optimized bridge case, the bond length between Ag and S atoms at the interface is 2.387 Å, which is close to the corresponding bond length in Ag_2S bulk, 2.47 Å.[27] We have also examined the effect of applied bias voltages on the stability of the three cases. As seen in the total energies calculated with fixing structural parameters except the *d* shown in Figure 2b, the bridge case remains lowest in total energy even in the cases with applied bias voltages.

The Mulliken charge distribution calculated self-consistently for the unrelaxed bridge case is shown in Figure 3. Only a small amount of charge, approximately 0.05 electrons per two-dimensional unit cell, is transferred from the Ag electrode to the Ag_2S layers at each interface, as in the case of the Fe−MgO−Fe sandwich system.[30] We can see clearly from Figure 3 that the charge variation due to the formation of the interface decays rapidly as the distance from the interface becomes larger, and the entire interfacial region is essentially neutral. It should be noted that there is a little polarization within the Ag_2S, that is, S layers obtain electrons at the expense of the electron loss in Ag layers.

Next, the transmission spectra for the three unrelaxed cases of interface structures with the same contact distance of

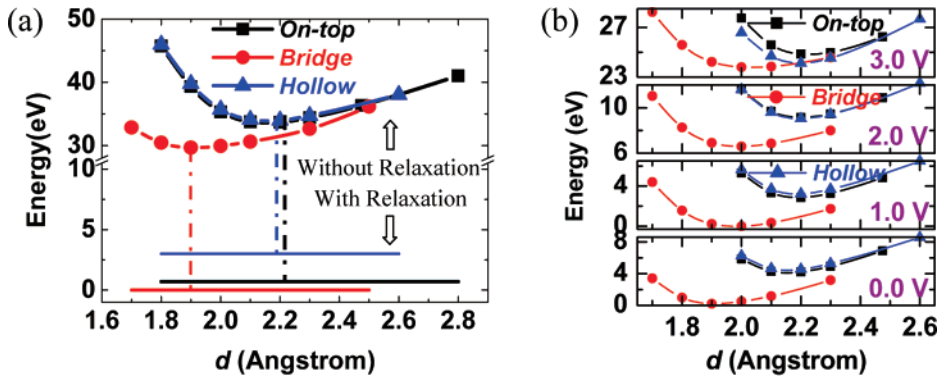

Figure 2. Calculated total energies as a function of the interlayer distance d between the Ag electrode and Ag_2S layer, for the three interface structures (a) without applying a bias voltage and (b) with applying bias voltages. Note that the curves in these figures are calculated with fixing structural parameters except d. In (a), the total energies calculated with full relaxation are also shown for d values corresponding to the minima of respective curves.

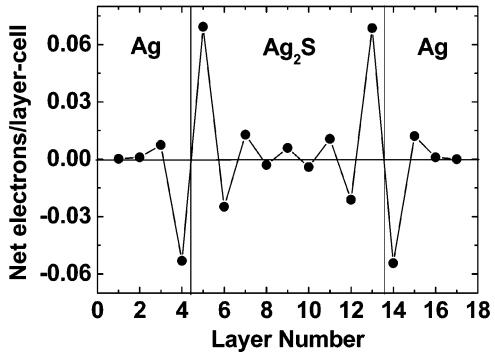

Figure 3. Mulliken charge distribution in the Ag−Ag_2S−Ag sandwich.

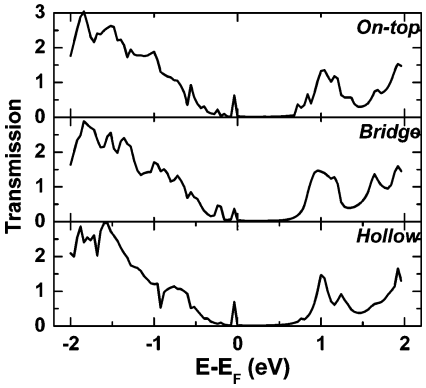

Figure 4. Transmission spectra of the three unrelaxed interface structures with the same contact distance of 2.0 Å. The Fermi level is set to zero.

2.0 Å are displayed in Figure 4a. The transmission spectra differ from one another suggesting the changes of electron states with interface structures. Common features seen in all the three interface structures are that the total transmission coefficients are almost zero in a region just above the Fermi level E_F and that the coefficient at E_F is very small, though it is finite ($\sim 0.04 \times 2\ e^2/\hbar$). This means electrons cannot permeate easily from the left Ag electrode to the right one. The "gap" in the transmission spectra can be attributed to the intrinsic semiconducting nature of Ag_2S.

The transmission spectra for structures of the bridge case having the lowest total energy with and without relaxation

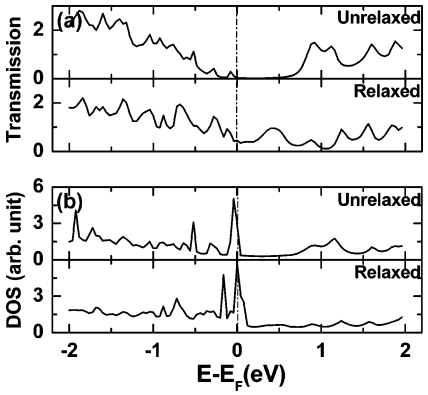

Figure 5. (a) Transmission spectra and (b) the total DOS, for the bridge case without and with structural relaxation under 0 V. The Fermi level is set to zero.

are shown in Figure 5a. The transmission coefficient at E_F increases from 0.04 before structural relaxation to 0.455 after relaxation, which shows the opening of a conduction channel in the relaxed structure. Moreover, the profiles of transmission spectra change drastically, which reflects sharp changes of electronic states in the sandwich system by the relaxation. From the density of states (DOS) shown in Figure 5b, we find that the huge increase in the DOS after structural relaxation makes transmission coefficient soar at E_F.

Investigation into atomic arrangement of the relaxed bridge structure reveals that a zigzag Ag atomic chain is formed in the Ag_2S. Atomic configuration of the Ag atomic chain and its electron density are illustrated in Figure 6. The neighboring Ag−Ag distances along the chain range from 2.84 to 3.07 Å (see numbers in Figure 6a), which are very near to the nearest neighbor distance in Ag bulk, 2.89 Å but deviate severely from Ag−Ag separation in the Ag_2S bulk, 3.08−3.74 Å.[27] Therefore, the zigzag Ag atomic chain is considered to play a crucial role in the rise of the transmission coefficient and DOS at E_F. Every atom along the chain except surface atoms of the electrodes has moved by approximately 1.2 Å in average during the process of the relaxation. This large displacement can be attributed to the influence of junction to the two electrodes, which may be enhanced by the large lattice mismatch between the Ag and Ag_2S in our model. The Ag_2S lattice constant is elongated by 15.2% along the

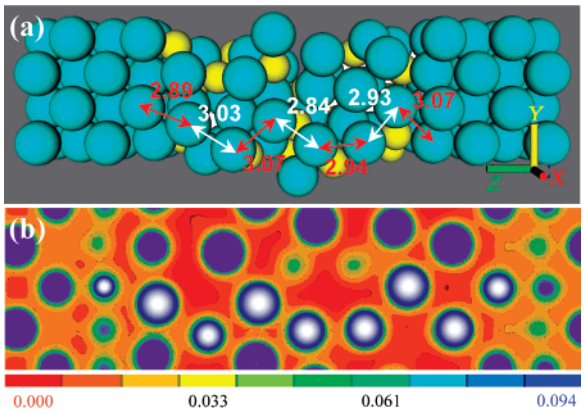

Figure 6. (a) Atomic arrangement of the relaxed structure of the bridge case under 0 V. The numbers denote the neighboring Ag−Ag distances along the chain in the Ag_2S. (b) Electron density corresponding to the atoms along the chain (represented by silvery balls).

x direction and compressed by 7.1% along the *y* direction to compensate the large mismatch of the interface constructed on the basis of the experimental report.[20,21] To clarify which of the two factors, the junction formation and the lattice mismatch, is dominant, calculations using models with larger size should be performed. Investigation of structural relaxation effects with such models, however, is impracticable at present because of huge computational cost and remains as a future task.

To confirm the role of the zigzag Ag chain more precisely, we considered a virtual system where all the atoms in the Ag_2S segment are removed from the relaxed bridge structure except Ag atoms in the chain and calculated the transmission between the Ag electrodes through this virtual chain. The calculated transmission coefficient at E_F is 0.967, which is in good agreement with the value calculated by Mozos et al. for an Ag wire.[31] It is worth noting that in their calculation, a zigzag arrangement of the Ag atoms is found to be energetically preferred and the optimized distance between atoms along the Ag chain is 2.78 Å. Our results are in accordance with theirs in both the shape of atomic chain and the interatomic distance. The difference of the transmission coefficient at E_F between the Ag−Ag_2S−Ag sandwich system and the virtual Ag chain system can be ascribed to the effect of other atoms in the Ag_2S on the Ag chain.

We also investigated the electronic and electric properties of the sandwich system under applied bias voltages. First, we calculated currents (*I*) under voltages (*V*) ranging from −3.0 to 3.0 V using the relaxed bridge structure. The *I*−*V* curve is nearly linear, showing the metallic nature of this system, which can be explained by the formation of the zigzag atomic chain. It is worth noting that the shape of the transmission spectra changes by applying bias voltages. This change, however, is not surprising because the application of bias voltage inevitably alters the effective potential in the scattering region. Next, we examined how the applied bias voltages drop along the Ag chain plane. Figure 7 illustrates the difference of the effective potential in the plane including the Ag chain between the case where the bias voltage of 0.5 V is applied and the case of 0.0 V, for both unrelaxed

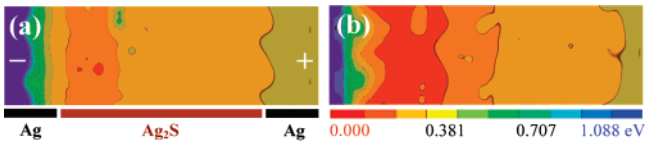

Figure 7. Difference of effective potential along the Ag chain plane by an applied bias voltage of 0.5 V for (a) an unrelaxed bridge case and (b) a relaxed bridge case.

and relaxed bridge cases. Note that, strictly speaking, the Ag chain is not in a plane, but we can say so roughly. One can see that intensive voltage drop takes place mainly around the negative bias end (left side) of the interface region, especially in the electrode area, for both cases. This concentration of the potential change due to the bias voltages around the negative bias end suggests that any change in the Ag_2S layer by applying bias voltage should commence from this area.[13,32] This is consistent with the speculation based on macroscopic electrochemistry that the formation of Ag switch starts from precipitation of Ag atoms near the negative electrode in the Ag_2S layer. We can also expect that forces in the *z* direction act on Ag atoms in the interface region by applying bias voltages (say, 0.21 eV/Å in average at 0.2 V). However, the displacements of the atoms by these forces are small, on the order of 0.02 Å at 0.2 V.

It should be noted that the mechanism of the "switch OFF" has not been discussed in the present study. Moreover, that of the "switch ON" state has hardly been discussed either, because the formation of the Ag chain without applying bias voltage is not directly related to the "switch ON" state. Further work to clarify the mechanisms is in progress. Nevertheless, we can say that the formation of the Ag chain found in the present study is instrumental for understanding the "switch ON" phenomenon. This suggests the possibility that in actual switches certain regions of the Ag_2S layer near the interface to electrodes may be conductive even in the "switch OFF" state. Then the length of the Ag bridge to be formed for the transition to the "switch ON" state may be shorter than the naive guess, that is, the thickness of the Ag_2S layer. Therefore, such spontaneous metallization at the Ag−Ag_2S interface may play an important role in fast switching of the Ag−Ag_2S atomic switch.

To conclude, we have examined electron transport and structural properties of the Ag_2S sandwiched between Ag electrodes, which models the nanoscale Ag−Ag_2S atomic switch using first-principles calculations. In the most stable structure we have examined, the transmission coefficient at the Fermi level increases sharply from 0.04 before structure optimization to 0.455 after structure optimization, showing the opening of a conductance channel. Furthermore, we have found that a zigzag Ag atomic chain is formed in the Ag_2S after relaxation, which is responsible for the increase in the transmission coefficient as well as the metallic behavior seen in the calculated current−voltage curve. We have also found that the potential change due to applied bias voltages mainly concentrates around the negative bias end of the interface region, which suggests that any change in the Ag_2S layer by applying bias voltage should commence from this area.

Acknowledgment. We thank Dr. Kazuya Terabe and Professor Shu Yamaguchi for useful discussions. This work was partially supported by the Grant-in-Aid for Scientific Research on Priority Area, "Nanoionics (439)", the Grant-in-Aid for Key-Technology, "Atomic Switch Programmed Device", and the Grant for 21st Century COE Program "Human-Friendly Materials based on Chemistry", by the Ministry of Education, Culture, Sports, Science and Technology.

References

(1) Metzger, R.; Chen, B.; Hopfner, U.; Lakshmikantham, M.; Vuillaume, D.; Kawai, T.; Wu, X.; Tachibana, H.; Hughes, T.; Sakurai, H.; Baldwin, J.; Hosch, C.; Cava, M.; Brehmer, L.; Ashwell, G. *J. Am. Chem. Soc.* **1997**, *19*, 10455.
(2) Chang, S. C.; Li, Z. C.; Lau, N.; Larade, B.; Williams, R. S. *Appl. Phys. Lett.* **2003**, *83*, 3198.
(3) Collier, C. P.; Wong, E. W.; Belohradsky, M.; Raymo, F. M.; Stoddart, J. F.; Kuekes, P. J.; Williams, R. S.; Heath, J. R. *Science* **1999**, *285*, 391.
(4) Collier, C. P.; Mattersteig, G.; Wong, E. W.; Luo, Y.; Beverly, K.; Sampaio, J.; Raymo, F. M.; Stoddart, J. F.; Heath, J. R. *Science* **2000**, *289*, 1172.
(5) Kuekes, P. J.; Stewart, D. R.; Williams, R. S. *J. Appl. Phys.* **2005**, *97*, 034301.
(6) Krans, J. M.; Van Ruitenbeek, J. M.; Fisun, V. V.; Yanson, J. K.; De Jongh, L. J. *Nature* **1995**, *375*, 767.
(7) Pascual, J. I.; Mendez, J.; Herrero, J. G.; Baro, A. M.; Garcia, N.; Binh, V. T. *Phys. Rev. Lett.* **1993**, *71*, 1852.
(8) Olesen, L.; Laegsgaard, E.; Stensgaard, I.; Besenbacher, F.; Schiotz, J.; Stoltze, P.; Jacobsen, K. W.; Norskov, J. K. *Phys. Rev. Lett.* **1994**, *72*, 2251.
(9) Rubio, G.; Agrait, N.; Vieira, S. *Phys. Rev. Lett.* **1996**, *76*, 2302.
(10) Li, J.; Speyer, G.; Sankey, O. F. *Phys. Rev. Lett.* **2004**, *93*, 248302.
(11) Zhang, C.; Du, M. H.; Cheng, H. P.; Zhang, X. G.; Roitberg, A. E.; Krause, J. L. *Phys. Rev. Lett.* **2004**, *92*, 158301.
(12) Taylor, J.; Guo, H.; Wang, J. *Phys. Rev. B* **2001**, *63*, R121104.
(13) Terabe, K.; Nakayama, T.; Hasegawa, T.; Aono, M. *J. Appl. Phys.* **2002**, *91*, 10110.
(14) Liang, C.; Terabe, K.; Hasegawa, T.; Negishi, R.; Tamura, T.; Aono, M. *Small* **2005**, *10*, 971.
(15) Terabe, K.; Nakayama, T.; Hasegawa, T.; Aono, M. *Appl. Phys. Lett.* **2002**, *80*, 4009.
(16) Terabe, K.; Hasegawa, T.; Nakayama, T.; Aono, M. *Nature* **2005**, *433*, 47.
(17) Grier, H.; Shapiro, S. M. *Phys. Rev. B* 1984, *29*, 3810.; Ray, J. R.; Vashishta, P. *J. Chem. Phys.* **1989**, *90*, 6580.
(18) Hull, S.; Keen, D. A.; Sivia, D. S.; Madden, P. A.; Wilson, M. *J. Phys.* 2002, *14*, L9. Andreoni, W. *Solid State Commun.* **1981**, *38*, 837.
(19) Kashida, S.; Watanabe, N.; Hasegawa, T.; Iida. H.; Mori, M.; Savrasov, S. *Solid State Ionics* **2003**, *158*, 167.
(20) Rivolta, B.; Lazzari, M.; Bicelli, L. P. *Gazz. Chim. Ital.* 1974, *104*, 179.
(21) Shiojiri, M.; Maeda, S.; Murata, Y. *J. Appl. Phys. Jpn.* **1969**, *8*, 24.
(22) Brandbyge, M.; Mozos, J.; Ordejon, P.; Taylor, J.; Stokbro, K. *Phys. Rev. B* **2002**, *65*, 165401.
(23) Taylor, J.; Guo, H.; Wang, J. *Phys. Rev. B* **2001**, *63*, 245407. Soler, J. M.; Artacho, E.; Gale, J. D.; Garcia, A.; Junquera, J.; Ordejon, P.; Daniel, S. *J. Phys.*: *Condens. Matter* **2002**, *14*, 2745. Taylor, J.; Brandbyge, M.; Stokbro, K. *Phys. Rev. Lett*. **2002**, *89*, 138301.
(24) Gutierrez, R.; Fagas, G.; Cuniberti, G.; Grossmann, F.; Schmidt, R.; Richter, K. *Phys. Rev. B* **2002**, *65*, 113410.
(25) Wu, X.; Li, Q.; Huang, J. *J. Chem. Phys.* **2005**, *123*, 184712.
(26) Troullier, N.; Martins, J. L. *Phys. Rev. B* **1991**, *43*, 1993.
(27) Sadanaga, R.; Sueno, S. *Mineral. J.* **1967**, *5*, 124.
(28) Junod, P.; Hediger, H.; Kilchor, B.; Wullschleger, J. *Philos. Mag.* **1977**, *36*, 941.
(29) Barman, S. R.; Shanthi, N.; Shukla, A. K.; Sarma, D. D. *Phys. Rev. B* **1996**, *53*, 3746.
(30) Butler, W. H.; Zhang, X.; Schulthess, T. C. *Phys. Rev. B* **2001**, *63*, 054416.
(31) Mozos, J. L.; Ordejon, P.; Brandbyge, M.; Taylor, J.; Stokbro, K. *Nanotechnology* **2002**, *13*, 346.
(32) Liang, C.; Terabe, K.; Hasegawa, T.; Aono, M. *Solid State Ionics* **2006**, *177*, 2527.

NL0711054